




Nontrivial intensity correlation from a coherent continuous-wave laser beam

Binod Joshi ^{*}, Thomas A. Smith [†], and Yanhua Shih 

Department of Physics, University of Maryland, Baltimore County, Baltimore, Maryland 21250, USA



(Received 6 May 2024; accepted 22 August 2024; published 4 September 2024)

We report an experimental observation of nontrivial intensity correlation of a continuous-wave fiber ring laser. The laser beam consists of approximately 450 000 independent longitudinal cavity modes, each in a coherent state representing a group of identical photons. Based on Glauber's second-order coherence theory, we conclude that the nontrivial intensity correlation is the result of a randomly created and randomly paired distinguishable group of identical photons interfering with the pair itself. This result is fundamentally interesting and practically useful.

DOI: [10.1103/PhysRevA.110.L031702](https://doi.org/10.1103/PhysRevA.110.L031702)

Since Hanbury Brown and Twiss (HBT) discovered intensity correlations in light from thermal (chaotic) sources, it is well accepted that intensity correlations, i.e., second-order coherence, can be used to characterize the quantum state of light [1–4]. Specifically, while light in a thermal state contains such correlations and is thus considered a correlated state, light in a coherent state, which is free from intensity fluctuations, does not produce correlations and is considered a noncorrelated state [5]. This Letter addresses the question: Can a multi-longitudinal-mode cw laser beam produce *nontrivial* intensity correlations as does the light in a thermal state? While such an inquiry is mainly aimed at fundamental understanding of the HBT phenomenon, its implications for quantum-inspired technologies may not be overlooked. Recently proposed quantum-correlation-based optical sensors may benefit from use of a bright laser beam as compared to a thermal light source [6–9]. Here, we report a recent experimental observation of nontrivial intensity correlation from the joint photodetection of such a laser beam.

The intensity correlation of radiation from lasers has been studied since the early days of laser physics [10,11, and references therein]. Tehrani and Mandel studied the correlations between the clockwise and counterclockwise propagating cavity modes of a ring laser, and concluded that “because the two counter-rotating modes of the ring laser compete partly for the same atomic population...the competition may...prevent it from reaching a coherent state, free from intensity fluctuations, that is generally regarded as the characteristic feature of a laser beam” [12]. The observed intensity correlation results from multimode lasers have been presented in literature as a result of “mode competition” preventing individual modes from reaching coherent states [13–22].

Interestingly, the results presented in this Letter show an HBT-type intensity correlation from a *coherent* multi-longitudinal-cavity-mode cw laser beam, henceforth written

as “multimode laser,” in the TEM₀₀ transverse mode. This signifies a differing mechanism from multimode lasers considered in the experimental demonstrations of the aforementioned literature. The multimode laser used for this measurement is a standard fiber ring laser consisting of an 8-m Erbium-doped single-mode optical fiber coupled into a 10-km single-mode fiber ring cavity. This laser generates approximately 450 000 longitudinal cavity modes, all in the TEM₀₀ transverse mode, and through stimulated emission each of these cavity modes produce a group of identical photons. We achieve an accurate match between experimental data and theoretical calculations for the second-order coherence function by using Glauber's quantum theory of optical coherence [23,24]. In our calculations, each individual group of photons is modeled as a coherent state, and the overall state of the laser output is a product of the 450 000 coherent states [25].

We begin our analysis with this theoretical discussion of the intensity correlation, i.e., the second-order coherence function, derived from Glauber's theory of photodetection. This is then followed by the details of our experimental scheme and the findings of the measurements.

Following Glauber's notation, we may consider the state of a cw laser beam with multilongitudinal modes [4,24]

$$|\Psi\rangle = \prod_m |\Psi_m\rangle = \prod_m |\alpha_m(\omega)\rangle, \quad (1)$$

where m labels the m th cavity mode, or the m th group of identical photons with frequency ω . The state $|\alpha_m(\omega)\rangle$ is an eigenstate of the annihilation operator with a complex eigenvalue $\alpha_m(\omega) = a_m(\omega)e^{i\phi_m(\omega)}$, which has a real and positive amplitude and a phase [26]

$$\hat{a}_m(\omega)|\alpha_m(\omega)\rangle = \alpha_m(\omega)|\alpha_m(\omega)\rangle. \quad (2)$$

Here, we make use of the coherent state representation for the state of a group of identical photons with $\bar{n} = |\alpha| \gg 1$, \bar{n} being the average number of identical photons in the coherent state.

The field operators for the measurements involved in our experiment, which are the quantum analogues of classical

^{*}Contact author: binodj1@umbc.edu

[†]Current address: Quantum Research and Applications Branch, Naval Air Warfare Center, Patuxent River, Maryland 20670, USA.

electric fields, are

$$\begin{aligned}\hat{E}^{(+)}(r_j, t_j) &= \sum_m \hat{a}_m(\omega) g_m(\omega; r_j, t_j) \\ \hat{E}^{(-)}(r_j, t_j) &= \sum_m \hat{a}_m^\dagger(\omega) g_m^*(\omega; r_j, t_j),\end{aligned}\quad (3)$$

where $j = 1, 2$; $g_m(\omega; r_j, t_j)$ is the Green's function that propagates the m th mode from the source to space-time coordinates (r_j, t_j) of the j th photodetector D_j . We have also ignored the constants.

The second-order coherence function, or correlation function, is thus [3,25,27]

$$\begin{aligned}G^{(2)}(r_1, t_1; r_2, t_2) &= \langle \hat{E}^{(-)}(r_1, t_1) \hat{E}^{(-)}(r_2, t_2) \hat{E}^{(+)}(r_2, t_2) \hat{E}^{(+)}(r_1, t_1) \rangle \\ &= \left\langle \sum_m \psi_m^*(r_1, t_1) \sum_n \psi_n^*(r_2, t_2) \right. \\ &\quad \left. \times \sum_q \psi_q(r_2, t_2) \sum_p \psi_p(r_1, t_1) \right\rangle\end{aligned}\quad (4)$$

Here, we have used

$$\begin{aligned}\langle \Psi | \hat{E}^{(+)}(r_j, t_j) | \Psi \rangle &= \langle \Psi | \sum_m \hat{a}_m(\omega) g_m(\omega; r_j, t_j) | \Psi \rangle \\ &= \sum_m \alpha_m(\omega) g_m(\omega; r_j, t_j) \\ &= \sum_m \psi_m(r_j, t_j),\end{aligned}\quad (5)$$

and defined $\psi_m(r_j, t_j)$ as the effective wave function of the m th “subfield”—an entity that consists of a large number of identical photons—that is measured by D_j [4,25].

Due to the random relative phases between the subfields, the only surviving terms in Eq. (4) are the $m = q$ and $n = p$ terms. So, we are left with

$$\begin{aligned}G^{(2)}(r_1, t_1; r_2, t_2) &= \sum_m \psi_m^*(r_1, t_1) \psi_m(r_1, t_1) \sum_n \psi_n^*(r_2, t_2) \psi_n(r_2, t_2) \\ &\quad + \sum_{m \neq n} \psi_m^*(r_1, t_1) \psi_n(r_1, t_1) \psi_n^*(r_2, t_2) \psi_m(r_2, t_2) \\ &= \sum_{m,n} \left| \frac{1}{\sqrt{2}} [\psi_m(r_1, t_1) \psi_n(r_2, t_2) + \psi_n(r_1, t_1) \psi_m(r_2, t_2)] \right|^2.\end{aligned}\quad (6)$$

Written in its final arrangement, this indicates the superposition of two different yet indistinguishable quantum probability amplitudes: (1) one or more identical photons from the m th longitudinal mode triggers D_1 at (r_1, t_1) while one or more identical photons from the n th longitudinal mode triggers D_2 at (r_2, t_2) ; and (2) one or more identical photons from the m th longitudinal mode triggers D_2 at (r_2, t_2) while one or more identical photons from the n th longitudinal mode triggers D_1 at (r_1, t_1) [28]. The second-order coherence function, or correlation function, of a multimode cw laser beam is thus the result of a nonlocal interference: a randomly created and

randomly paired distinguishable group of identical photons interfering with the pair itself [4].

In Eq. (6), the cross-interference term is the “nontrivial” contribution to the second-order coherence function $G^{(2)}(r_1, t_1; r_2, t_2)$, corresponding to the intensity fluctuation correlation (IFC) of the cw laser beam measured jointly by D_1 and D_2 ,

$$\begin{aligned}\langle \Delta I(r_1, t_1) \Delta I(r_2, t_2) \rangle &= \sum_{m \neq n} \psi_m^*(r_1, t_1) \psi_n(r_1, t_1) \psi_n^*(r_2, t_2) \psi_m(r_2, t_2),\end{aligned}\quad (7)$$

while the product of the mean intensities measured by each photodetector is

$$\begin{aligned}\langle I(r_1, t_1) \rangle \langle I(r_2, t_2) \rangle &= \sum_m \psi_m^*(r_1, t_1) \psi_m(r_1, t_1) \sum_n \psi_n^*(r_2, t_2) \psi_n(r_2, t_2).\end{aligned}\quad (8)$$

The normalized $G^{(2)}(r_1, t_1; r_2, t_2)$ is thus related to the intensity fluctuation correlation as

$$g^{(2)}(r_1, t_1; r_2, t_2) \propto 1 + \frac{\langle \Delta I(r_1, t_1) \Delta I(r_2, t_2) \rangle}{\langle I(r_1, t_1) \rangle \langle I(r_2, t_2) \rangle}.\quad (9)$$

In the calculations so far, we have assumed an idealized, true single-frequency cavity mode. Realistically, we may have to take into account the finite spectral bandwidth of a cavity mode with the following integral:

$$\begin{aligned}\psi_m(r_j, t_j) &= \int_{\Delta\omega} d\omega \alpha_m(\omega) g_m(\omega; r_j, t_j) \\ &\simeq \left[\int_{\Delta\nu} d\nu \alpha_m(\nu) e^{-i\nu\tau_{mj}} \right] e^{-i\omega_m\tau_j} \\ &= \mathcal{F}_{\tau_{mj}} \{a(\nu)\} e^{-i\omega_m\tau_j},\end{aligned}\quad (10)$$

where we have assumed a point-to-point free propagation. $\nu = \omega - \omega_m$ is the detuning frequency from the central frequency ω_m of the m th cavity mode, and $a(\nu)$ is the spectral function of the cavity mode. Here, each cavity mode has been modeled as a wave packet with carrier frequency ω_m and an “envelope,” which is the Fourier transform of the spectral distribution function of the m th mode. We have also introduced the notations $\tau_j \equiv t_j - r_j/c$ and $\tau_{mj} = \tau_j - t_m$, where t_m is the emission time of the m th cavity mode.

With this model of the cavity modes, we now calculate the intensity fluctuation correlation [as clarified in Eq. (7), this calculation deals with the case $m \neq n$]:

$$\begin{aligned}\langle \Delta I(\tau_1) \Delta I(\tau_2) \rangle &= \sum_{m,n} \mathcal{F}_{\tau_{1m}}^* \{a(\nu)\} e^{i\omega_m\tau_1} \mathcal{F}_{\tau_{1n}} \{a(\nu)\} e^{-i\omega_n\tau_1} \\ &\quad \times \mathcal{F}_{\tau_{2n}}^* \{a(\nu)\} e^{i\omega_n\tau_2} \mathcal{F}_{\tau_{2m}} \{a(\nu)\} e^{-i\omega_m\tau_2} \\ &= \left[\sum_m \mathcal{F}_{\tau_{1m}}^* \{a(\nu)\} \mathcal{F}_{\tau_{2m}} \{a(\nu)\} e^{i\omega_m\tau} \right] \\ &\quad \times \left[\sum_n \mathcal{F}_{\tau_{1n}} \{a(\nu)\} \mathcal{F}_{\tau_{2n}}^* \{a(\nu)\} e^{-i\omega_n\tau} \right],\end{aligned}\quad (11)$$

where $\tau \equiv \tau_1 - \tau_2 = (t_1 - t_2) - (r_1 - r_2)/c$. Calculating one summation at a time, we find

$$\begin{aligned} & \sum_m \mathcal{F}_{\tau_{1m}}^* \{a(v)\} \mathcal{F}_{\tau_{2m}} \{a(v)\} e^{i\omega_m \tau} \\ & \simeq \int dt_m \mathcal{F}_{\tau_{1m}}^* \{a(v)\} \mathcal{F}_{\tau_{2m}} \{a(v)\} \\ & \quad \times [e^{i\omega_1 \tau} [1 + e^{i\omega_b \tau} + e^{i2\omega_b \tau} + \dots + e^{i(N-1)\omega_b \tau}]] \\ & \simeq \mathcal{F}_\tau \{a^2(v)\} \left[e^{i(N-1)\omega_b \tau/2} \frac{\sin(N\omega_b \tau/2)}{\sin(\omega_b \tau/2)} \right]. \end{aligned} \quad (12)$$

Here ω_b is the *beat* frequency between neighboring cavity modes and N is the total number of cavity modes. The cross-interference term then reduces to

$$\langle \Delta I(\tau_1) \Delta I(\tau_2) \rangle \propto |\mathcal{F}_\tau \{a^2(v)\}|^2 \left[\frac{\sin^2(N\omega_b \tau/2)}{\sin^2(\omega_b \tau/2)} \right]. \quad (13)$$

Here, $N\omega_b$ is the total range of frequencies present. If electronic response times are slow relative to the range of optical beat frequencies present, they result in a time average that contributes to the broadening of the measured correlation function.

The second part of the product in Eq. (13) representing the correlation peaks is independent of the choice of the distribution function $a(v)$ for each cavity mode. In other words, the “envelope” over the correlation peaks, given by the Fourier transform, does not have any impact on the internal structure or spacing of the correlation peaks themselves, other than defining their common profile. In general, the distribution function $a(v)$ for each cavity mode may be approximated to as any form, such as Gaussian or Lorentzian. To use a simple case as an example, we can model $a(v)$ as an approximately constant distribution (i.e., a rectangular function) for each cavity mode within its spectral bandwidth $\Delta\omega$. Equation (13) then results in

$$\langle \Delta I(\tau_1) \Delta I(\tau_2) \rangle \propto \text{sinc}^2 \left(\frac{\Delta\omega\tau}{2} \right) \frac{\sin^2(N\omega_b \tau/2)}{\sin^2(\omega_b \tau/2)}, \quad (14)$$

where, again, $\Delta\omega$ is the spectral bandwidth, or linewidth, of the cavity mode; ω_b is the beat frequency between neighboring cavity modes; and $\tau \equiv \tau_1 - \tau_2$. Figure 1 shows two plots of the normalized correlation function $g^{(2)}$ [which is related to the IFC via Eq. (9)] with a sinc^2 profile. The plots are generated with the same values of N and ω_b but different $\Delta\omega$. It is clear that the bandwidth of the individual longitudinal modes determines the width of the sinc^2 envelope and, thus, whether it can be measured within a given temporal range. Note that the choice of the distribution function $a(v)$ as well as the associated parameters used to generate the plots in Fig. 1 are arbitrary and are meant for illustrative purposes. These do not necessarily represent the laser system in our experimental arrangement to be discussed later in this report. Additionally, it should be noted that achieving a maximum value of 2 in the measurement of the normalized correlation may be contingent on experimental conditions.

The setup of our experiment is schematically illustrated in Fig. 2. The radiation source is a laboratory-assembled fiber laser consisting of a laser controller (not shown in the figure), an erbium doped fiber amplifier (EDFA), and a single-mode fiber ring cavity with adjustable length. The EDFA, in

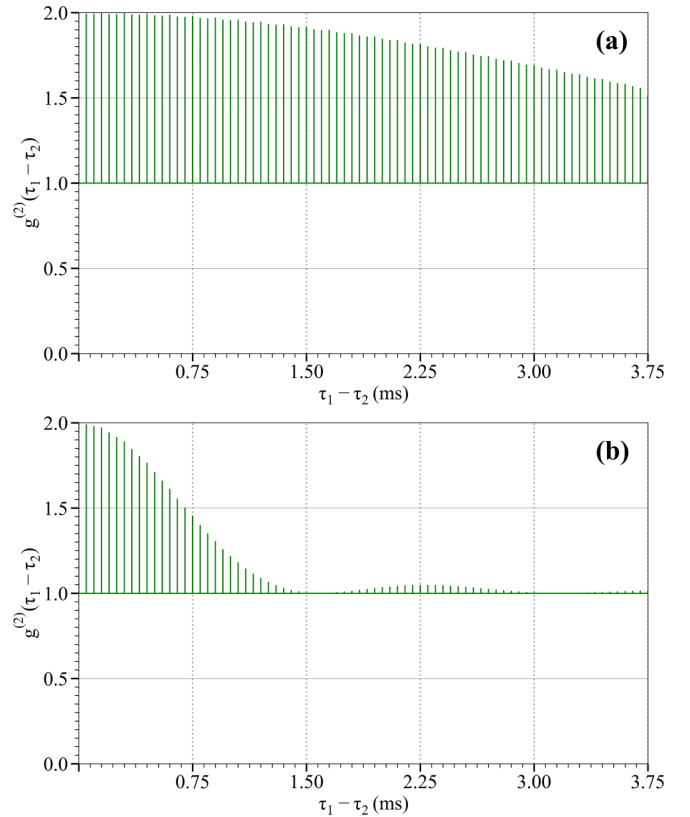


FIG. 1. Theoretical plots of the normalized correlation function $g^{(2)}$ of Eq. (9), based on the result of Eq. (14); taking $N = 100\,000$ and beat frequency $(\omega_b/2\pi) = 20$ kHz. The optical delay $r_1 - r_2$ has been chosen to be 0, so that the time delays $\tau_1 - \tau_2$ and $t_1 - t_2$ represent the same quantity. (a) Mode width $(\Delta\omega/2\pi) = 35$ Hz; (b) mode width = 200 Hz.

combination with the ring cavity, is used to generate multimode continuous-wave laser beam. Only one of the two outputs, either clockwise or counterclockwise, of the ring cavity is used for the intensity correlation measurement. The laser beam is passed through a fiber beamsplitter and fed into two identical point-like analog photodetectors D_1 and D_2 , each of which has a response spectrum bandwidth of 5 GHz. The output photocurrents of the photodiodes, $i_1(t_1) \propto I_1(t_1)$ and $i_2(t_2) \propto I_2(t_2)$, together with their registration times t_1 and t_2 , are processed by the measurement scheme which involves a combination of a state-of-the-art digitizing oscilloscope with high real-time bandwidth and a computer for the postprocessing of the data to get the intensity correlation as a function of $t_1 - t_2$.

The laser is designed to give a maximum output power of 5 mW, with a maximum pump power of 10 mW, while the threshold pump power is approximately 0.38 mW. For the measurements presented in this report, the pump power was chosen to be in the range 1.4–1.8 mW, far above the threshold of the laser for reaching a coherent state. The power level of 1.8 mW is also far below the maximum pump power (and hence the maximum output power of the fiber laser) to avoid any possible mode locking. The intensity measurement of the laser beam shows an approximately constant signal without any pulses, as expected for the cw operation. The power

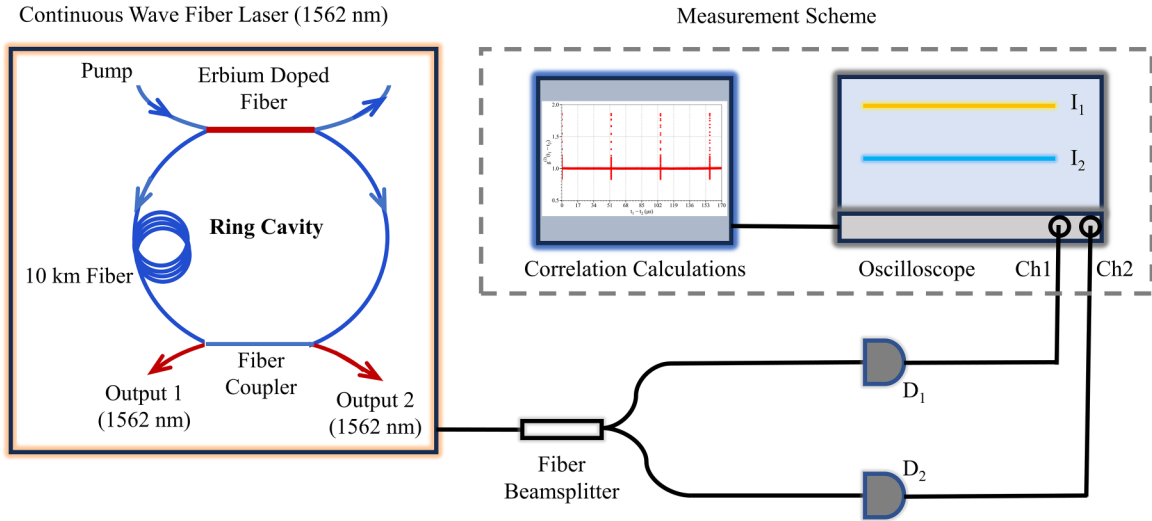


FIG. 2. Schematic setup for intensity correlation measurement of a multimode fiber laser. D_1 and D_2 are two analog photodiodes, and Ch1 and Ch2 are corresponding input channels of the digital oscilloscope.

spectrum recorded by an optical spectrum analyzer (OSA) as depicted in Fig. 3 shows that the spectral profile of the TEM₀₀ laser beam has a FWHM bandwidth $\Delta\lambda \simeq 0.07$ nm ($\Delta f \simeq 8.6$ GHz), with the spectrum peak being in the telecom C band (in the range of 1562–1563 nm). The presence of smaller peaks in the spectrum was found to be caused by polarization inhomogeneities; hence, a fiber polarization controller was used to ensure that the main peak remains dominant in the spectrum. Single-mode fiber optic launch cables optimized for minimum loss in the wavelength range of the laser, ranging from a few meters to kilometers in length, were used in our measurements to generate different cavity lengths for testing the setup and verifying the theoretical results. In this report, the ring cavity length was chosen to be 10.69 km. For this ring cavity, the theoretically expected value of mode separation is $\omega_b/2\pi = 19.12$ kHz [29]. Using the laser bandwidth of 8.6 GHz measured by the OSA, this gives a calculated value of $N = 449\,790$, which we approximate as $N \simeq 450\,000$.

The intensity correlation measurement without the use of optical delay is presented in Fig. 4. This result is, in fact,

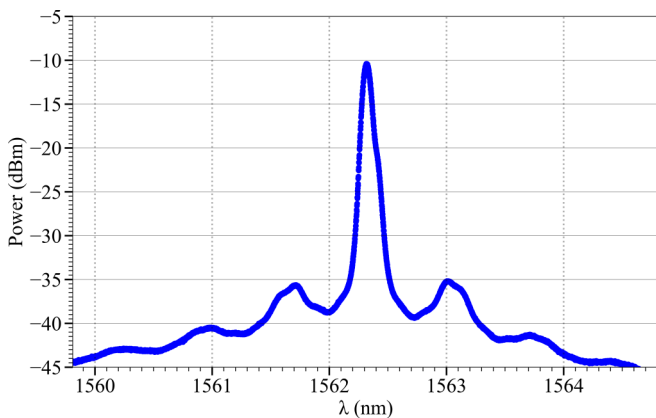


FIG. 3. Typical spectral profile of the laser beam, as observed on an optical spectrum analyzer.

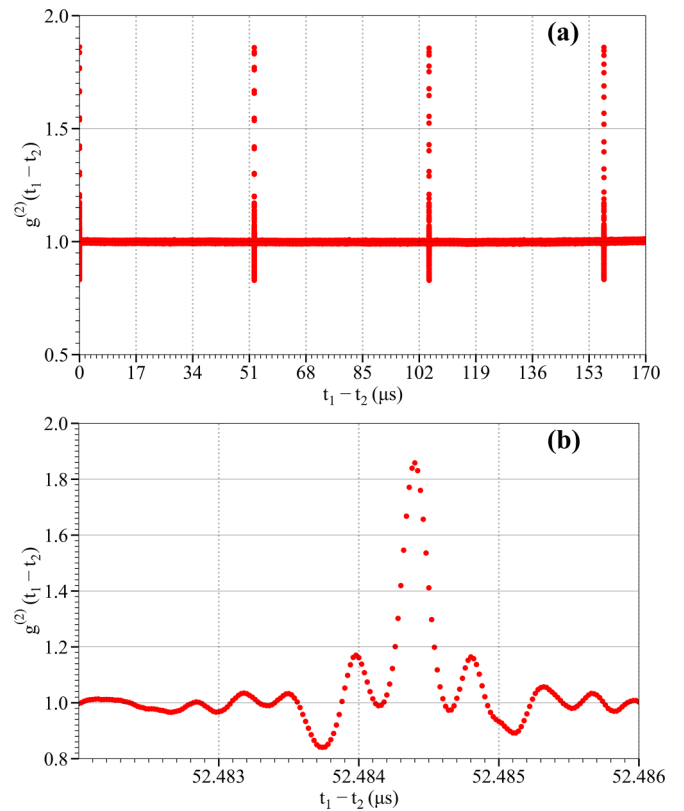


FIG. 4. Typical temporal correlation measurements for the setup in Fig. 2 for 10.69-km cavity length and zero optical delay ($r_1 - r_2 = 0$). The y axis is $g^{(2)}(t_1 - t_2)$, which is related to the intensity fluctuation correlation by Eq. (9). (a) The first peak is located at $t_1 - t_2 = 0$, as expected for a measurement with no optical delay; while the second peak is around 52.48 μs , thus giving a beat period of 52.48 μs which is equivalent to the beat frequency of 19.05 kHz. The subsequent peaks also maintain this beat period of 52.48 μs . (b) Detailed view of the second peak demonstrating its structure and a higher precision of its temporal location.

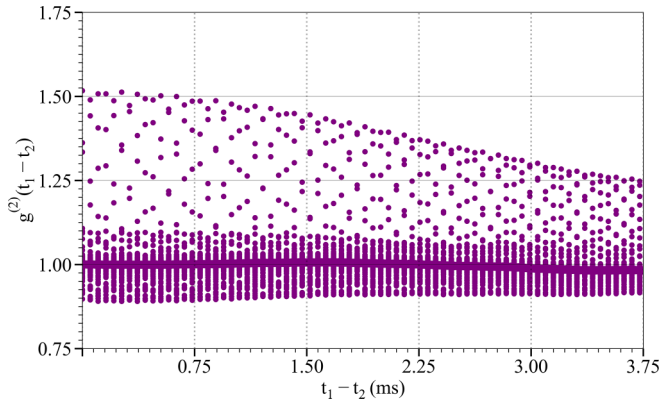


FIG. 5. Typical profile of the correlation peaks, related to the “envelope” described by Eq. (13) for the setup in Fig. 2 for 10.69-km cavity length and zero optical delay. The maximum observable temporal range is limited by the measurement scheme. The slight deviation of the baseline of the peaks (representing the trivial part of the correlation function) from a perfectly horizontal line may be ascribed to random sources of instabilities in the laser spectrum.

the measure of the normalized second-order coherence, or correlation, function $g^{(2)}(t_1 - t_2)$. It is clearly observed that the correlation function consists of distinct peaks described by the second term of Eq. (13), representing the intensity fluctuation correlation, with an average period of 52.48 μs , equivalent to a beat frequency of 19.05 kHz. This value is close to the theoretical estimate of 19.12 kHz. The peaks protruding downward from the baseline are the artifacts resulting from the convolution effect originating from the finite temporal response of the photodetectors. The FWHM of an individual peak was found to be 180 ps, with accuracy limited by the sampling resolution of the oscilloscope as well as the bandwidth and temporal response of the photodetectors.

For a separate set of measurements done over a longer temporal range (limited only by the sampling features of

the oscilloscope), we observed the presence of an envelope over these peaks. A typical result is shown in Fig. 5. The ability to observe the complete profile in a typical correlation measurement being considered in this work is affected by the bandwidth of the individual modes, as was depicted previously in the example of Fig. 1. Hence, the data presented in Fig. 5 implies that the mode width for our laser system was too narrow to be observed with the measurement scheme being employed. While the nature of the curve describing this envelope could not be determined with certainty due to the aforementioned limitations, it is reasonable to conclude that its functional form can, in principle, be modeled by the Fourier transform of a suitable distribution function $a(\nu)$ of the modes.

In summary, we demonstrated an HBT-type intensity correlation of a multimode cw laser beam. The laser generates a large number ($\sim 450\,000$) of longitudinal cavity modes with TEM₀₀ transverse profile, each containing a large number of identical photons. The state of each cavity mode can be represented as a coherent state, and the state of the laser output is thus a product of the $\sim 450\,000$ coherent states. Based on Glauber’s second-order coherence theory, we conclude that the observed nontrivial intensity correlation is the result of a randomly paired distinguishable group of identical photons interfering with the pair itself. Our results provide a positive answer to the fundamental question: Can a coherent cw laser beam produce intensity correlation like thermal light? In addition to being fundamentally interesting, a bright light source of cw laser beam with HBT-type intensity correlation can be useful for quantum technologies.

We would like to thank M. F. Locke, A. Katz, L. Yan, and M. M. Fitelson for providing us with necessary equipment and helpful suggestions. The generous support provided by Z. Zhang for computing resources is also acknowledged. This work was partially supported by Northrop Grumman Corporation and Naval Air Warfare Center Aircraft Division.

- [1] R. H. Brown and R. Q. Twiss, *Nature (London)* **177**, 27 (1956).
- [2] R. H. Brown and R. Q. Twiss, *Nature (London)* **178**, 1046 (1956).
- [3] M. O. Scully and M. S. Zubairy, *Quantum Optics* (Cambridge University Press, Cambridge, 1997).
- [4] Y. H. Shih, *An Introduction to Quantum Optics: Photon and Biphoton Physics*, 2nd ed. (CRC Press, Boca Raton, 2021).
- [5] L. Mandel and E. Wolf, *Optical Coherence and Quantum Optics* (Cambridge University Press, Cambridge, 1995).
- [6] G. Scarcelli, A. Valencia, and Y. H. Shih, *Europhys. Lett.* **68**, 618 (2004).
- [7] Y. S. Ihn, Y. Kim, V. Tamma, and Y.-H. Kim, *Phys. Rev. Lett.* **119**, 263603 (2017).
- [8] T. A. Smith and Y. H. Shih, *Phys. Rev. Lett.* **120**, 063606 (2018).
- [9] C.-H. Lee, Y. Kim, D.-G. Im, U.-S. Kim, V. Tamma, and Y.-H. Kim, *Phys. Rev. Lett.* **131**, 223602 (2023).
- [10] D. E. McCumber, *Phys. Rev.* **141**, 306 (1966).
- [11] H. Risken, in *Progress in Optics*, edited by E. Wolf (Elsevier, New York, 1970), Vol. 8, pp. 239–294.
- [12] M. M. Tehrani and L. Mandel, *Phys. Rev. A* **17**, 677 (1978).
- [13] T. Aoki, Y. Endo, and K. Sakurai, *Opt. Commun.* **23**, 26 (1977).
- [14] F. T. Hioe, *J. Math. Phys.* **19**, 1307 (1978).
- [15] F. T. Hioe, S. Singh, and L. Mandel, *Phys. Rev. A* **19**, 2036 (1979).
- [16] W. Brunner and H. Paul, *Opt. Quant. Electron.* **15**, 87 (1983).
- [17] C. Tremblay and R. Maciejko, *IEEE Photon. Technol. Lett.* **2**, 100 (1990).
- [18] J. Kinoshita and T. Aoki, *Phys. Rev. A* **46**, 5938 (1992).
- [19] M. Lebedev, A. Demenev, A. Parakhonsky, and O. Misochko, *Optics* **3**, 46 (2022).
- [20] S. K. Turitsyn, S. A. Babin, D. V. Churkin, I. D. Vatnik, M. Nikulin, and E. V. Podivilov, *Phys. Rep.* **542**, 133 (2014).
- [21] A. S. Gomes, A. L. Moura, C. B. de Araújo, and E. P. Raposo, *Prog. Quantum Electron.* **78**, 100343 (2021).
- [22] E. P. Raposo, I. R. R. González, E. D. Coronel, A. M. S. Macêdo, L. d. S. Menezes, R. Kashyap, A. S. L. Gomes, and R. Kaiser, *Phys. Rev. A* **105**, L031502 (2022).
- [23] R. J. Glauber, *Phys. Rev. Lett.* **10**, 84 (1963).

- [24] R. J. Glauber, *Phys. Rev.* **131**, 2766 (1963).
- [25] R. J. Glauber, *Phys. Rev.* **130**, 2529 (1963).
- [26] For a cw laser, the relative phases between cavity modes are random numbers. For a cw-mode locked laser, the relative phases between cavity modes can be constant, resulting in pulses.
- [27] R. Loudon, *The Quantum Theory of Light* (Oxford University Press, New York, 2000).
- [28] U. Fano, *Am. J. Phys.* **29**, 539 (1961).
- [29] O. Svelto, *Principles of Lasers* (Springer, New York, 2010).